

# Crystal Structures and $^{29}\text{Si}$ NMR Calculations of Amino-Functionalized Silyllithium Compounds

Carsten Strohmann,<sup>\*,[a]</sup> Oliver Ulbrich,<sup>[a]</sup> and Dominik Auer<sup>[a]</sup>

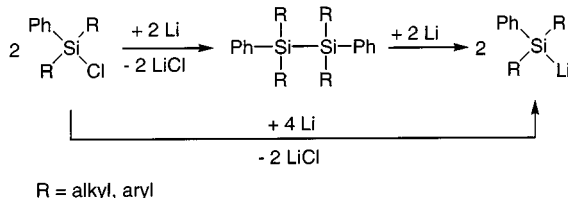
**Keywords:** Ab initio calculations / Lithium / NMR spectroscopy / Silanes / Si ligands

X-ray structural analysis of the amino-functionalized silyllithium compounds tris(tetrahydrofuran)[bis(diethylamino)phenylsilyl]lithium (**4**·3THF) and tris(tetrahydrofuran)[(diethylamino)bisphenylsilyl]lithium (**7**·3THF) are presented. Both compounds are monomeric in the solid state as well as in solution. Despite the formal negative charge at the silicon atom, the nitrogen centres are flattened. No Li–N interactions were observed, in contrast to the homologous (lithiomethyl)amines. RI-DFT calculations give an explanation for the variation of experimental Si–Li bond lengths of 2.627(4) Å

(**4**·3THF), 2.682(8) Å (**7**·3THF) and 2.732(7) Å {tris(tetrahydrofuran)[bis(diphenylamino)phenylsilyl]lithium} (**1**·3THF). N–Si orbital interactions, influenced by the type of substituents located at the nitrogen centre, affect these structural parameters as well as the  $^{29}\text{Si}$  NMR chemical shifts. The apparently unusual experimental values of the  $^{29}\text{Si}$  NMR resonance signals at  $\delta = 20.3$  (for **7**·3THF) and  $\delta = 28.4$  (for **4**·3THF) can be explained by DFT-IGLO calculations and are a consequence of the combination of electronegative and electropositive substituents at the silicon centre.

## Introduction

Silyllithium compounds are useful and important reagents for silyl-group transfer reactions to organic molecules or organometallic systems.<sup>[1a,1b]</sup> Generally, silyllithiums can be prepared by reaction of a chlorosilane with lithium metal and cleavage of the disilane intermediate (Scheme 1),<sup>[2a–2c]</sup> although that method is limited to systems bearing at least one aryl group.<sup>[2c]</sup>



Scheme 1.

In contrast to alkyl- and arylsilyllithiums, functionalized silyllithium species have been studied less extensively. Some dialkylamino-functionalized silyllithium compounds with phenyl substituents at the central silicon atom have been developed by Tamao et al.<sup>[3a–3c]</sup> These compounds, especially **4** and **7**, can be prepared according to Scheme 1 and are stable in solution at room temperature. Nevertheless, structural information about these dialkylamino-functionalized silyllithium compounds is scarce.<sup>[4a,4b,5]</sup> Tamao and co-workers were able to prove that dialkylamino-functionalized silyllithiums are monomeric in solution by observation of  $^{29}\text{Si}$ – $^7\text{Li}$  coupling (quadruplet) in the  $^{29}\text{Si}$  NMR spectra in the temperature range of  $-100$  to  $-110$  °C.<sup>[5]</sup> However, the nature of the unusual  $^{29}\text{Si}$  NMR chemical

shifts of such compounds is still not well understood. More structural information about dialkylamino-functionalized silyllithiums can be concluded from the solid state structure of tris(tetrahydrofuran)[(diphenylamino)bisphenylsilyl]lithium (**1**·3THF) (Figure 1).<sup>[5]</sup>

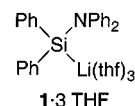


Figure 1. Structural formula of **1**·3THF

The crystal structure shows a monomeric silyllithium system with the lithium centre being coordinated by three THF molecules. A closer look at the structural parameters reveals a quite long Si–Li bond of 2.732(7) Å and a planar nitrogen centre. The phenyl substituents at the nitrogen centre enhance the planarisation of this centre, and therefore it is not clear if this system is comparable to the synthetically useful dialkylamino-functionalized silyllithiums. Elongation of the Si–Li and Si–N bonds in compound **1**·3THF should be caused by the additional interaction of the lone pair at the amino group with the phenyl substituents.

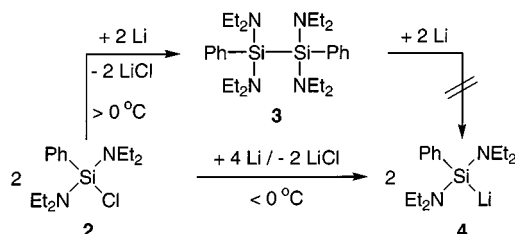
We attach importance to the clarification of the structural facts of dialkylamino-functionalized silyllithiums in order to study structure/reactivity patterns. The most important questions are: i) What are the structures of bis(diethylamino)phenylsilyllithium (**4**) or (diethylamino)bisphenylsilyllithium (**7**) in the solid state? and ii) How can we explain the unusual downfield shifts of the  $^{29}\text{Si}$  NMR resonance signals?<sup>[3a,5]</sup>

## Results and Discussion

The silyllithium compound **4** was prepared starting from chlorosilane **2** and lithium metal in THF, as described by

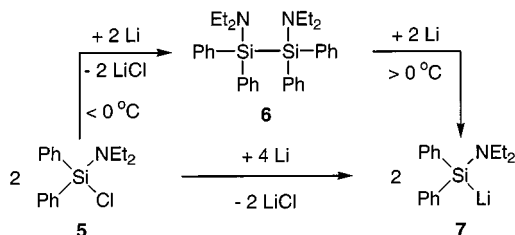
<sup>[a]</sup> Institut für Anorganische Chemie, Universität Würzburg  
Am Hubland, 97074 Würzburg, Germany  
Fax: (internat.) +49-931/888-4605  
E-mail: c.strohmamm@mail.uni-wuerzburg.de

Tamao and co-workers (Scheme 2).<sup>[3c]</sup> In the  $^{29}\text{Si}$  NMR spectrum of the reaction mixture of **2** with lithium metal at temperatures above  $0^\circ\text{C}$  we observe a resonance signal for the disilane **3** (main product), as well as a signal for **4**. Furthermore we also found chlorosilane **2** at shorter reaction times, allowing us to conclude that the reaction of **2** with **4** to give **3** is slow. Disilane **3** is not cleaved by lithium to give the silyllithium compound **4**. We assume the following reaction pathway: the silyllithium compound **4** is the primary product of the reaction of chlorosilane **2** with lithium metal, compound **4** reacts to form the disilane **3** at temperatures above  $0^\circ\text{C}$  and a cleavage of the disilane by lithium is not observed. Reaction of **2** at low temperatures ( $< 0^\circ\text{C}$ ) leads to **4**, which is stable and does not react with chlorosilane **2** at that temperature.



Scheme 2.

The analogous synthesis of the silyllithium species **7**, also described by Tamao and co-workers,<sup>[3c]</sup> follows a different reaction path (Scheme 3). The primary product of the reaction of chlorosilane **5** with lithium metal at temperatures of  $-40$  to  $-20^\circ\text{C}$  is the disilane **6**. Raising the temperature of the reaction mixture to  $0^\circ\text{C}$  results in the cleavage of the Si–Si bond and the formation of the silyllithium species **7**. This can also be recognized by a change of colour during the reaction or from the analogous synthesis of **7** starting from **6**.



Scheme 3.

Compounds **4** and **7** were isolated as crystalline THF adducts. The amino-functionalized silyllithium compound **4**·3THF crystallized from *n*-pentane at  $-90^\circ\text{C}$  in the triclinic crystal system, space group  $P\bar{1}$  (Figure 2 and Table 2). The crystals melt at temperatures above  $-20^\circ\text{C}$ . **4**·3THF is monomeric in the solid state with the lithium centre being surrounded by three THF molecules in a tetrahedral geometry. Neither an intramolecular coordination of the lithium centre by the nitrogen atoms nor a chelating effect could be observed. This is not unusual but *is* in contrast to (lithiomethyl)amines.<sup>[6]</sup> Nevertheless the Si–Li bond length is relatively short [2.627(4) Å] compared to other silyllithium species [2.732(7) Å in **1**·3THF;<sup>[5]</sup> 2.70 Å in  $(\text{Me}_3\text{SiLi})_2 \cdot 3 (\text{Me}_2\text{NCH}_2\text{CH}_2\text{NMe}_2)_3$ ;<sup>[7]</sup> 2.66 Å in

$(\text{Me}_3\text{Si})_3\text{SiLi} \cdot 3\text{THF}$ ;<sup>[8]</sup> 2.67 Å in  $\text{Ph}_3\text{SiLi} \cdot 3\text{THF}$ ;<sup>[9]</sup> 2.65 Å in  $(\text{Me}_3\text{SiLi})_6$ ].<sup>[10a,10b]</sup> The two nitrogen centres in **4**·3THF show an almost planar environment; the deviations from the plane are 0.057 and 0.088 Å. The total sum of the bond angles at the nitrogen centres are  $354.9^\circ$  and  $358^\circ$ , respectively ( $360^\circ$  in **1**·3THF<sup>[5]</sup>). The Si–N bond lengths in **4**·3THF are relatively long [1.772(2) and 1.781(2) Å] compared to other aminosilanes [1.73 and 1.72 Å in  $(\text{Et}_2\text{N})_2\text{PhSiSiPh}(\text{NEt}_2)_2$ ],<sup>[11]</sup> but shorter than the corresponding bonds of 1.824(3) Å in **1**·3THF (see Table 1).

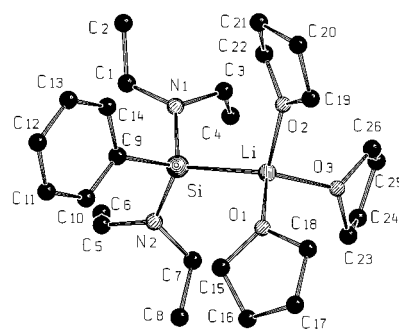


Figure 2. Molecular structure of tris(tetrahydrofuran)[bis(diethylamino)phenylsilyl]lithium (**4**·3THF) in the crystal; selected bond lengths [Å] and angles [ $^\circ$ ]: Si–Li 2.627(4), Si–N(1) 1.781(2), Si–N(2) 1.772(2), Si–C(9) 1.926(2), Li–O(1) 1.987(5), Li–O(2) 1.972(5), Li–O(3) 1.971(4); N(2)–Si–N(1) 112.66(11), N(2)–Si–C(9) 100.14(11), N(1)–Si–C(9) 100.01(11), N(2)–Si–Li 120.05(13), N(1)–Si–Li 110.26(13), C(9)–Si–Li 111.39(12), C(1)–N(1)–C(3) 113.4(2), C(1)–N(1)–Si 124.9(2), C(3)–N(1)–Si 116.6(2), C(7)–N(2)–C(5) 114.2(2), C(7)–N(2)–Si 119.0(2), C(5)–N(2)–Si 124.8(2).

Crystals from the amino-functionalized silyllithium compound **7**·3THF could be obtained by fast crystallization from a solution in *n*-pentane at  $-30^\circ\text{C}$ . The compound crystallises in the monoclinic crystal system, space group  $P2_1/c$  with two molecules in the asymmetric unit (Figure 3 and 4, and Table 2). The structure analysis was performed at  $-10^\circ\text{C}$ , because single crystals of **7**·3THF are very sensitive to strong cooling, which results in a slow decomposition and bad quality of the collected reflection data. Like **4**·3THF the silyllithium species **7**·3THF is monomeric in the solid state and no intramolecular coordination of the lithium centre by the nitrogen atom was found. The lithium centres are surrounded by three THF molecules in a tetrahedral geometry. The Si–Li bond lengths [2.682(8) and 2.678(8) Å] are longer than in the comparable compound **4**·3THF. An elongation of the Si–N bond relative to other aminosilanes can also be observed. The nitrogen centre shows an almost planar environment, as in compound **4**·3THF, with deviations from the plane of 0.061 and 0.095 Å and a sum of angles of  $357.6^\circ$  and  $354.1^\circ$ , respectively.

The structure of **4**·3THF in  $[\text{D}_8]\text{toluene}$  solution is also monomeric, which is confirmed by an observed  $^{29}\text{Si}$ – $^7\text{Li}$  coupling [quadruplet for the resonance signal,  $^1J(^{29}\text{Si}, ^7\text{Li}) = 56.8 \text{ Hz}$ ] in the  $^{29}\text{Si}$  NMR spectrum at  $-40^\circ\text{C}$ . Further cooling causes an asymmetric spreading and a splitting of the signal set at  $-75^\circ\text{C}$  indicating a freezing of a dynamic process. Compound **7**·3THF also shows monomeric behav-

Table 1. Selected data taken from crystal structure analysis and quantum chemical calculations

	1·3THF <sup>[5]</sup>	Crystal structure analysis		1·3THF	Calculated values <sup>[a]</sup>	
		4·3THF	7·3THF		4·3THF	7·3THF
Si–Li [Å]	2.732(7)	2.627(4)	2.682(8) 2.678(8)	2.770	2.680	2.732
Si–N [Å]	1.824(3)	1.781(2) 1.772(2)	1.764(4) 1.763(4)	1.873	1.837 1.827	1.824
N (Sum of angles) [°]	360.0	354.9/358	357.6/354.1	360.0	354.8/357.9	354.0

<sup>[a]</sup> Values taken from RI-DFT calculations at the BP86/TZVP level.

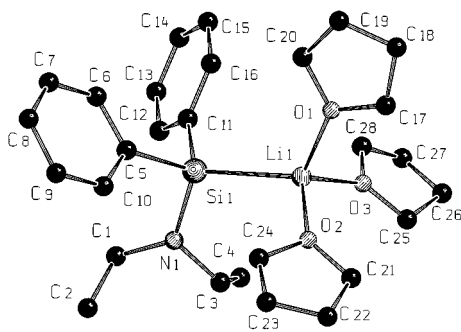


Figure 3. Molecular structure of tris(tetrahydrofuran)[(diethylamino)bisphenylsilyl]lithium (**7·3THF**) (molecule 1) in the crystal; selected bond lengths [Å] and angles [°]: Si(1)–Li(1) 2.682(8), Si(1)–N(1) 1.764(4), Si(1)–C(5) 1.909(5), Si(1)–C(11) 1.917(5), Li(1)–O(1) 1.966(10), Li(1)–O(2) 1.944(9), Li(1)–O(3) 1.978(10); N(1)–Si(1)–C(5) 100.7(2), N(1)–Si(1)–C(11) 106.3(2), N(1)–Si(1)–Li(1) 109.2(2), C(5)–Si(1)–Li(1) 123.4(2), C(11)–Si(1)–Li(1) 115.2(2), C(5)–Si(1)–C(11) 100.1(2), C(1)–N(1)–C(3) 112.8(5), C(1)–N(1)–Si(1) 125.8(4), C(3)–N(1)–Si(1) 119.0(4)

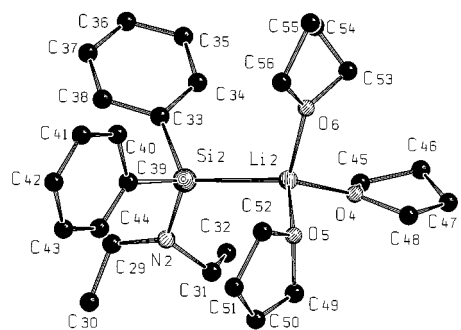


Figure 4. Molecular structure of tris(tetrahydrofuran)[(diethylamino)bisphenylsilyl]lithium (**7·3THF**) (molecule 2) in the crystal; selected bond lengths [Å] and angles [°]: Si(2)–Li(2) 2.678(8), Si(2)–N(2) 1.763(4), Si(2)–C(33) 1.926(4), Si(2)–C(39) 1.916(5), Li(2)–O(4) 1.954(9), Li(2)–O(5) 1.969(9), Li(2)–O(6) 1.970(9); N(2)–Si(2)–C(33) 106.0(2), N(2)–Si(2)–C(39) 101.6(2), N(2)–Si(2)–Li(2) 116.4(2), C(33)–Si(2)–Li(2) 119.2(2), C(39)–Si(2)–Li(2) 111.4(2), C(33)–Si(2)–C(39) 99.7(2), C(29)–N(2)–C(31) 112.9(4), C(29)–N(2)–Si(2) 122.4(3), C(31)–N(2)–Si(2) 118.8(3)

our in [D<sub>8</sub>]toluene solution. At –68 °C a <sup>29</sup>Si–<sup>7</sup>Li coupling [quadruplet for the resonance signal, <sup>1</sup>*J*(<sup>29</sup>Si, <sup>7</sup>Li) = 50.6 Hz] can be observed in the <sup>29</sup>Si NMR spectrum. Further cooling does not lead to an asymmetric spreading as in compound **4·3THF**. These <sup>29</sup>Si–<sup>7</sup>Li couplings do not allow us to reach any definite conclusion about the nature of the Si–Li bond (contribution of covalency), although it is conspicuous that lithiated silanes with coordinating solvents

show a directed Si–Li interaction<sup>[7–10b]</sup> in contrast to the alkyl homologues.<sup>[12]</sup>

Comparing the structures of the dialkylaminosilyllithium compounds **4·3THF** and **7·3THF** with other structural data from known silyllithium compounds shows, that the Si–Li bonds are among the shortest [2.627 (4) Å for **4·3THF**] and the longest [2.732(7) Å for **1·3THF**] of such systems. In order to distinguish between crystallographic (e.g. packing) and substituent effects at the silicon centre we performed quantum chemical calculations on compounds **1·3THF**, **4·3THF** and **7·3THF**. RI-DFT calculations at the BP86/TZVP level were used for structure optimization of these molecules. The relative values of important structural parameters, such as Si–Li and Si–N distances, are reproduced by these quantum chemical calculations (see Table 1). The performed DFT calculations overestimate the values of the bond lengths, as is common for such methods.<sup>[13a,13b]</sup>

NBO analyses show that the lone pair of the dialkylamino group interacts with an antibonding orbital located at the silicon centre, resulting in an increase in the charge at this centre compared to triorganosilyllithium compounds. These interactions cause a contraction of the polar Si–Li bond and therefore **4·3THF** has the shortest Si–Li distance of all three systems. Since **7·3THF** has only one dialkylamino group, the Si–Li bond length is longer than in **4·3THF**. The lone pair at the nitrogen centre in **1·3THF** is delocalized onto the phenyl groups; this results in a weaker interaction with the silicon centre and therefore the Si–N and Si–Li bonds are elongated.

Tamao and co-workers observed that the <sup>29</sup>Si NMR spectra of (aminosilyl)lithiums and (alkoxysilyl)lithiums show a downfield shift relative to the corresponding chlorosilanes, in contrast to (triorganosilyl)lithiums.<sup>[3a,5]</sup> In order to understand these downfield shifts and the observed structural parameters we optimized the energy of the simplified model compounds Ph(Me<sub>2</sub>N)<sub>2</sub>SiLi and Ph<sub>2</sub>(Me<sub>2</sub>N)SiLi by DFT methods [B3LYP/6–31+G(d)] and calculated the NMR resonance signals using the GIAO method [HF/6–311+G(2d,p)].<sup>[14a,14b]</sup> The geometrical parameters of the minimized model systems show similar structural characteristics as the molecular structures of **4·3THF** and **7·3THF** in the crystal, but with too short Si–Li bonds [2.476 Å for Ph(Me<sub>2</sub>N)<sub>2</sub>SiLi and 2.490 Å for Ph<sub>2</sub>(Me<sub>2</sub>N)SiLi]. This effect can be explained by the absence of coordinating solvent molecules. The calculated values for the <sup>29</sup>Si NMR resonance signals of our model compounds are δ = 21.0

[Ph(Me<sub>2</sub>N)<sub>2</sub>SiLi] and  $\delta = 18.9$  [Ph<sub>2</sub>(Me<sub>2</sub>N)SiLi], close to the experimental values of  $\delta = 28.4$  for **4** and  $\delta = 20.3$  for **7**. These results confirm the trend of the downfield shift of functionalized silyllithiums compared to (triorgano)silyllithiums, and therefore coordinating solvent molecules can be omitted in model systems for <sup>29</sup>Si NMR calculations.

Calculations performed on the simplified model systems Me<sub>3</sub>SiLi, Me<sub>2</sub>(H<sub>2</sub>N)SiLi and Me(H<sub>2</sub>N)<sub>2</sub>SiLi within the bounds of the DFT-IGLO method allow a thorough analysis of the shielding tensors concerning paramagnetic contributions of localised molecular orbitals (LMO).<sup>[15a,15b]</sup> The result is that, with the change from Me<sub>3</sub>SiLi (calculated chemical shift:  $\delta = -5.7$ ) to Me<sub>2</sub>(H<sub>2</sub>N)SiLi (calculated chemical shift:  $\delta = 14.9$ ), the significant contribution for the shielding tensors of the remaining two LMOs of the Si–C bond as well as the Si–Li LMO increase considerably. This is caused by the very large induced coupling of these LMOs with the  $\sigma^*(\text{Si–N})$  orbital, resulting in a decreased shielding [and increased chemical shift of Me<sub>2</sub>(H<sub>2</sub>N)SiLi]. At the same time the number of Si–C LMOs decreases (Si–N LMOs make a lower paramagnetic contribution than Si–C LMOs). The latter effect predominates with the addition of a second H<sub>2</sub>N group [Me(H<sub>2</sub>N)<sub>2</sub>SiLi] causing, in total, an increase of the shielding compared to Me<sub>2</sub>(H<sub>2</sub>N)SiLi [calculated chemical shift for Me(H<sub>2</sub>N)<sub>2</sub>SiLi:  $\delta = 9.9$ ]. A similar trend was observed for the gradual replacement of the methyl groups of Me<sub>4</sub>Si with chloro substituents.<sup>[16]</sup> That effect can also be observed for other metallated silanes with R<sub>2</sub>N or RO substituents and explained by NMR calculations. Further calculations on this topic are in progress.

## Experimental Section

**General:** All preparations were performed using standard Schlenk techniques under an oxygen-free and water-free argon atmosphere. Tetrahydrofuran was dried over Na/benzophenone and freshly distilled under argon. <sup>29</sup>Si NMR spectra were recorded on a Bruker DRX-300 (59.6 MHz) spectrometer with an external standard of tetramethylsilane ( $\delta = 0.0$ ).

**Synthesis of Tris(tetrahydrofuran)[bis(diethylamino)phenylsilyl]lithium (**4**·3THF):** The synthesis was performed as described by Tamao and co-workers<sup>[3c]</sup> but with a reaction temperature of  $-40$  to  $-20$  °C. – <sup>29</sup>Si{<sup>1</sup>H} NMR (C<sub>7</sub>D<sub>8</sub>, 233 K):  $\delta = 28.4$  (q, <sup>1</sup>J<sub>SiLi</sub> = 56.8 Hz).

**Synthesis of Tris(tetrahydrofuran)[(diethylamino)biphenylsilyl]lithium (**7**·3THF):** The synthesis was performed as described by Tamao and co-workers<sup>[3c]</sup>. – <sup>29</sup>Si{<sup>1</sup>H} NMR (C<sub>7</sub>D<sub>8</sub>, 205 K):  $\delta = 20.3$  (q, <sup>1</sup>J<sub>SiLi</sub> = 50.6 Hz).

**Computational Methods:** All calculations were carried out on gas-phase structures.<sup>[17]</sup> Structure optimizations of Ph(Me<sub>2</sub>N)<sub>2</sub>SiLi and Ph<sub>2</sub>(Me<sub>2</sub>N)SiLi at the B3LYP/6–31+G(d) level were performed using GAUSSIAN 98.<sup>[14b]</sup> Selected bond lengths [Å] and angles [°] for Ph(Me<sub>2</sub>N)<sub>2</sub>SiLi: Si–Li 2.481, Si–N(1) 1.788, Si–N(2) 1.788, Si–C(5) 1.922, C(5)–Si–N(1) 102.8, C(5)–Si–N(2) 102.8, N (sum over angles) 355.0; absolute SCF energy:  $-797.855415745$  Hartree; – selected bond lengths [Å] and angles [°] for Ph<sub>2</sub>(Me<sub>2</sub>N)SiLi:

Si–Li 2.490, Si–N 1.786, Si–C(3) 1.921, Si–C(9) 1.934, C(3)–Si–N 104.3, C(9)–Si–N 108.5, N (sum over angles) 352.4; absolute SCF energy:  $-894.925802514$  Hartree.

The RI-DFT<sup>[18]</sup> calculations on compounds **1**·3THF, **4**·3THF and **7**·3THF were done with the TURBOMOLE<sup>[19]</sup> program at the BP86/TZVP level with starting coordinates taken from the crystal structure analyses. Selected bond lengths [Å] and angles [°] for **1**·3THF: Si–Li 2.770, Si–N 1.873, Si–C(1) 1.950, Si–C(7) 1.939, C(1)–Si–N 103.4, C(7)–Si–N 103.9, N (sum over angles) 360.0; absolute SCF energy:  $-1976.437591873$  Hartree; – selected bond lengths [Å] and angles [°] for **4**·3THF: Si–Li 2.688, Si–N(1) 1.827, Si–N(2) 1.837, Si–C(9) 1.948, C(9)–Si–N(1) 100.8, C(9)–Si–N(2) 100.5, N (sum over angles) 357.9; absolute SCF energy:  $-1653.02345787$  Hartree; – selected bond lengths [Å] and angles [°] for **7**·3THF: Si–Li 2.732, Si–N 1.824, Si–C(5) 1.964, Si–C(11) 1.947, C(5)–Si–N 105.8, C(11)–Si–N 101.4, N (sum over angles) 354.0; absolute SCF energy:  $-1671.469514876$  Hartree. The criterion for convergence for these calculations was lowered to a change in absolute SCF energy of  $5 \times 10^{-5}$  Hartree, due to the size of these systems. Minimizing the energy starting from the second conformer of **7**·3THF in the crystal showed no significant differences in the results compared to the calculated values of the other conformer of **7**·3THF.

The GIAO method-based NMR calculations [HF/6–311+G(2d,p)] of Ph(Me<sub>2</sub>N)<sub>2</sub>SiLi and Ph<sub>2</sub>(Me<sub>2</sub>N)SiLi were performed with GAUSSIAN 98.<sup>[14a,14b]</sup> Calculated absolute shieldings  $\sigma$  were converted into relative shifts  $\delta$  with  $\sigma$  calculated at the same level for TMS [ $\sigma_{\text{calcd}}(\text{Si}) = 385.9$ ]; calculated value of  $\sigma$  for Ph(NMe<sub>2</sub>)<sub>2</sub>SiLi: 364.83; calculated value of  $\sigma$  for Ph<sub>2</sub>(NMe<sub>2</sub>)SiLi: 367.18.

The structures of the model systems Me<sub>3</sub>SiLi, Me<sub>2</sub>(H<sub>2</sub>N)SiLi and Me(H<sub>2</sub>N)<sub>2</sub>SiLi were optimized at the B3LYP/6–31+G(d) level using GAUSSIAN 98.<sup>[14b]</sup> Selected bond lengths [Å] and angles [°] for Me<sub>3</sub>SiLi: Si–Li 2.516, Si–C 1.928, C–Si–C 104.2, C–Si–Li 114.4; absolute SCF energy:  $-416.770639118$  Hartree; selected bond lengths [Å] and angles [°] for Me<sub>2</sub>(H<sub>2</sub>N)SiLi: Si–Li 2.509, Si–C(1) 1.921, Si–C(2) 1.930, Si–N 1.790, C(1)–Si–N 101.9, C(2)–Si–N 109.8; absolute SCF energy:  $-432.828715216$  Hartree; selected bond lengths [Å] and angles [°] for Me(H<sub>2</sub>N)<sub>2</sub>SiLi: Si–Li 2.494, Si–C 1.915, Si–N(1) 1.788, Si–N(2) 1.788, C–Si–N(1) 100.5, C–Si–N(2) 100.6; absolute SCF energy:  $-448.891440368$  Hartree. DFT-IGLO calculations of chemical shifts for Me<sub>3</sub>SiLi, Me<sub>2</sub>(H<sub>2</sub>N)SiLi and Me(H<sub>2</sub>N)<sub>2</sub>SiLi have been done at the sum-over-states density-functional perturbation theory level (SOS-DFPT),<sup>[15b,20]</sup> varying the gradient-corrected PW91<sup>[21a–21c]</sup> exchange-correlation functional. A compromise strategy discussed earlier<sup>[15b,22a,22b]</sup> was applied to obtain accurate Kohn–Sham MOs with moderate effort, by adding an extra iteration with a larger integration grid and without fit of the exchange-correlation potential after SCF convergence had been reached. FINE<sup>[22a,22b]</sup> angular grids with 32 points of radial quadrature were used. All of the DFT-IGLO calculations were carried out using the deMon NMR code.<sup>[22a,22b,23]</sup> IGLO-II all-electron basis sets were used on all atoms with density and exchange-correlation potential fitting auxiliary basis sets of the sizes 5.1 (H), 5.2 (C, Li, N) and 5.4 (Si). Calculated absolute shieldings  $\sigma$  were converted into relative shifts  $\delta$  with  $\sigma$  calculated at the same level for TMS [ $\sigma_{\text{calcd}}(\text{Si}) = 368.1$ ]. Absolute shielding  $\sigma$  and selected contributions of certain LMOs for Me<sub>3</sub>SiLi:  $\sigma = 373.8$ , Si–C LMO  $-100.5$ , Si–Li LMO  $-103.7$ ; absolute shielding  $\sigma$  and selected contributions of certain LMOs for Me<sub>2</sub>(H<sub>2</sub>N)SiLi:  $\sigma = 353.2$ , Si–C(1) LMO  $-116.0$ , Si–C(2) LMO  $-111.2$ , Si–N LMO  $-91.0$ , lone pair N LMO 7.4, Si–Li



Table 2. Selected crystallographic data for 4·3THF and 7·3THF

	4·3THF	7·3THF
Empirical formula	C <sub>26</sub> H <sub>49</sub> LiN <sub>2</sub> O <sub>3</sub> Si	C <sub>28</sub> H <sub>44</sub> LiNO <sub>3</sub> Si
Formula weight [g/mol]	472.70	477.67
Temperature [K]	173(2)	263(2)
Wavelength [Å]	0.71073	0.71073
Crystal system	Triclinic	Monoclinic
Space group	<i>P</i> 1	<i>P</i> 2 <sub>1</sub> / <i>c</i>
<i>a</i> [Å]	8.981(2)	10.274(2)
<i>b</i> [Å]	10.424(2)	33.791(7)
<i>c</i> [Å]	17.668(4)	17.996(4)
$\alpha$ [°]	74.36(3)	90
$\beta$ [°]	76.67(3)	103.14(3)
$\gamma$ [°]	67.16(3)	90
Volume [Å <sup>3</sup> ]	1453.1(5)	6084.1(22)
<i>Z</i>	2	8
Density (calcd.) [g/cm <sup>3</sup> ]	1.080	1.043
<i>F</i> (000)	520	2080
Crystal size [mm <sup>3</sup> ]	0.60 × 0.40 × 0.20	0.80 × 0.80 × 0.50
Theta range for data collection [°]	2.26 to 27.00	2.40 to 24.00
Index ranges ( <i>h</i> , <i>k</i> , <i>l</i> )	−11,11; −13,13; −23,23	−13,13; −44,43; −23,23
Reflections collected	10362	30076
Independent reflections	5922 [ <i>R</i> (int) = 0.0616]	9344 [ <i>R</i> (int) = 0.1266]
Refinement method	Full-matrix least-squares on <i>F</i> <sup>2</sup>	
Data/restraints/parameters	5913/0/302	9333/0/618
Goodness-of-fit on <i>F</i> <sup>2</sup>	1.008	1.050
Final <i>R</i> indices [ <i>I</i> > 2σ( <i>I</i> )]	<i>R</i> 1 = 0.0606	<i>R</i> 1 = 0.0832
	<i>wR</i> 2 = 0.1450	<i>wR</i> 2 = 0.1927
	<i>R</i> 1 = 0.1048	<i>R</i> 1 = 0.1701
	<i>wR</i> 2 = 0.1680	<i>wR</i> 2 = 0.2216
<i>R</i> indices (all data)	—	0.0019(7)
Extinction coefficient	—	0.306 and −0.300
Largest diff. peak and hole [eÅ <sup>−3</sup> ]	0.422 and −0.361	—

LMO −120.0; absolute shielding  $\sigma$  and selected contributions of certain LMOs for Me(H<sub>2</sub>N)<sub>2</sub>SiLi:  $\sigma$  = 358.2, Si–C LMO −116.3, Si–N(1) LMO −85.6, lone pair N(1) −3.6, Si–N(2) LMO −100.6, lone pair N(2) LMO 4.5, Si–Li LMO −126.9.

**X-ray Crystal Structure Analysis:** Suitable crystals of 4·3THF and 7·3THF were obtained from *n*-pentane solutions at −30 °C (7·3THF) or −90 °C (4·3THF) as THF adducts. The crystals were mounted in inert oil on a glass fibre and transferred to the cold gas stream of the diffractometer [Stoe IPDS; graphite monochromated Mo-*K*<sub>α</sub> radiation ( $\lambda$  = 0.71073 Å)]. The structures were solved using direct and Fourier methods (SHELXS-86<sup>[24a]</sup>); refinement by full-matrix least-squares methods (based on *F*<sub>o</sub><sup>2</sup>, SHELXL-93<sup>[24b]</sup>); anisotropic thermal parameters for all non-H atoms in the final cycles; the H atoms were refined on a riding model in their ideal geometric positions. Crystal data and refinement details of structures 4·3THF and 7·3THF are reported in Table 2.

Crystallographic data (excluding structure factors) for the structures included in this paper have been deposited with the Cambridge Crystallographic Data Centre as supplementary publication nos. CCDC-139102 (4·3THF) and -151411 (7·3THF). Copies of the data can be obtained free of charge on application to CCDC, 12 Union Road, Cambridge CB2 1EZ, UK [Fax: (internat.) + 44-1223/336-033; Email: deposit@ccdc.cam.ac.uk].

## Acknowledgments

We are grateful to the Deutsche Forschungsgemeinschaft (DFG), the Fonds der Chemischen Industrie and Chemetall GmbH for financial support and the donation of chemicals. We thank Prof. Dr. M. Kaupp, Universität Würzburg, for helpful discussions regarding the interpretations of the NMR calculations.

[1] [1a] I. Fleming, R. S. Roberts, S. C. Smith, *J. Chem. Soc., Perkin*

- Trans. 1* **1998**, 1215–1228. — [1b] U. Schubert, A. Schenkel, *Transition Met. Chem.* **1985**, 210–212.
- [2] [2a] N. A. Rahman, I. Fleming, A. B. Zwicky, *J. Chem. Res. (S)* **1992**, 292. — [2b] H. Gilman, K. Shiina, D. Aoki, B. J. Gaj, D. Wittenberg, T. Brennan, *J. Organomet. Chem.* **1968**, 13, 323–328. — [2c] K. Tamao, A. Kawachi, *Adv. Organomet. Chem.* **1995**, 38, 1–58.
- [3] [3a] A. Kawachi, K. Tamao, *Bull. Chem. Soc. Jpn.* **1997**, 70, 945–955; selected <sup>29</sup>Si NMR spectroscopic data of alkylsilyllithium-, aminosilyllithium- and alkoxy-silyllithium compounds and the corresponding chlorosilanes: Ph<sub>2</sub>MeSiCl ( $\delta$  = 10.0), Ph<sub>2</sub>MeSiLi ( $\delta$  = −20.5), (Et<sub>2</sub>N)PhMeSiCl ( $\delta$  = 2.3), (Et<sub>2</sub>N)PhMeSiLi ( $\delta$  = 14.4), (Et<sub>2</sub>N)<sub>2</sub>PhSiCl ( $\delta$  = −18.8), (Et<sub>2</sub>N)<sub>2</sub>PhSiLi ( $\delta$  = 28.7), (*t*BuO)<sub>2</sub>PhSiCl ( $\delta$  = −56.5), (*t*BuO)<sub>2</sub>PhSiLi ( $\delta$  = 41.8). — [3b] K. Tamao, A. Kawachi, Y. Ito, *Organometallics* **1993**, 12, 580–582. — [3c] K. Tamao, A. Kawachi, Y. Tanaka, H. Ohtani, Y. Ito, *Tetrahedron* **1996**, 52, 5765–5772.
- [4] [4a] A. Kawachi, K. Tamao, 12th International Symposium on Organosilicon Chemistry, Sendai, Japan, poster abstracts P 82. — [4b] C. Strohmman, O. Ulbrich, 12th International Symposium on Organosilicon Chemistry, Sendai, Japan, poster abstracts P 81.
- [5] A. Kawachi, K. Tamao, *J. Am. Chem. Soc.* **2000**, 122, 191–196.
- [6] C. Bruhn, F. Becke, D. Steinborn, *Organometallics* **1998**, 17, 2124–2126.
- [7] B. Teclé, W. H. Ilsley, J. P. Oliver, *Organometallics* **1982**, 1, 875–877.
- [8] A. Heine, R. Herbst-Irmer, G. M. Sheldrick, D. Stalke, *Inorg. Chem.* **1993**, 32, 2694–2698.
- [9] H. V. R. Dias, M. M. Olmstead, K. Ruhlandt-Senge, P. P. Power, *J. Organomet. Chem.* **1993**, 462, 1–6.
- [10] [10a] T. F. Schaaf, W. Butler, M. D. Glick, J. P. Oliver, *J. Am. Chem. Soc.* **1974**, 96, 7593–7594. — [10b] W. H. Ilsley, T. F. Schaaf, M. Glick, J. P. Oliver, *J. Am. Chem. Soc.* **1980**, 102, 3769–3774.
- [11] K. Tamao, A. Kawachi, Y. Nakagawa, Y. Ito, *J. Organomet. Chem.* **1994**, 473, 29–34.
- [12] T. Kottke, D. Stalke, *Angew. Chem.* **1993**, 105, 619–621; *Angew. Chem. Int. Ed. Engl.* **1993**, 32, 580–582.

- [13] [13a] M. Kaupp, *Chem. Ber.* **1996**, *129*, 535–544. — [13b] J. A. Altmann, N. C. Handy, V. E. Ingamells, *Int. J. Quant. Chem.* **1996**, *57*, 533–542.
- [14] [14a] K. Wolinski, J. F. Hilton, P. Pulay, *J. Am. Chem. Soc.* **1990**, *112*, 8251–8260. — [14b] Gaussian 98; Revision A.6, M. J. Frisch, G. W. Trucks, H. B. Schlegel, G. E. Scuseria, M. A. Robb, J. R. Cheeseman, V. G. Zakrzewski, J. A. Montgomery, Jr., R. E. Stratmann, J. C. Burant, S. Dapprich, J. M. Millam, A. D. Daniels, K. N. Kudin, M. C. Strain, O. Farkas, J. Tomasi, V. Barone, M. Cossi, R. Cammi, B. Mennucci, C. Pomelli, C. Adamo, S. Clifford, J. Ochterski, G. A. Petersson, P. Y. Ayala, Q. Cui, K. Morokuma, D. K. Malick, A. D. Rabuck, K. Raghavachari, J. B. Foresman, J. Cioslowski, J. V. Ortiz, B. B. Stefanov, G. Liu, A. Liashenko, P. Piskorz, I. Komaromi, R. Gomperts, R. L. Martin, D. J. Fox, T. Keith, M. A. Al-Laham, C. Y. Peng, A. Nanayakkara, C. Gonzalez, M. Challacombe, P. M. W. Gill, B. Johnson, W. Chen, M. W. Wong, J. L. Andres, C. Gonzalez, M. Head-Gordon, E. S. Replogle, and J. A. Pople, Gaussian, Inc., Pittsburgh PA, **1998**.
- [15] [15a] W. Kutzelnigg, U. Fleischer, M. Schindler, in *NMR-Basic Principles and Progress*, Vol. 23, Springer, Heidelberg, **1990**, pp. 165ff. — [15b] V. G. Malkin, O. L. Malkina, L. A. Eriksson, D. R. Salahub, in *Theoretical and Computational Chemistry*, Vol. 2 (Eds.: P. Politzer, J. M. Seminario), Elsevier, Amsterdam, **1995**.
- [16] S. Berger, W. Bock, G. Frenking, V. Jonas, F. Müller, *J. Am. Chem. Soc.* **1995**, *117*, 3820–3829.
- [17] *Landolt-Börnstein, Numerical Data and Functional Relationships in Sciences and Technology*, Vols 7, 15, 21, 23: *Structure Data of Free Polyatomic Molecules*, Springer, Berlin, **1979**, **1987**, **1992**, **1995**.
- [18] K. Eichkorn, O. Treutler, H. G. Öhm, M. Häser, R. Ahlrichs, *Chem. Phys. Lett.* **1995**, *240*, 283–289.
- [19] Program System TURBOMOLE V 5.1: R. Ahlrichs, M. Bär, M. Häser, H. Horn, C. Kömel, *Chem. Phys. Lett.* **1989**, *162*, 165–169.
- [20] V. G. Malkin, O. L. Malkina, M. E. Casida, D. R. Salahub, *J. Am. Chem. Soc.* **1994**, *116*, 5898–5908.
- [21] [21a] J. P. Perdew, Y. Wang, *Phys. Rev. B* **1992**, *45*, 13244–13249. — [21b] J. P. Perdew, in *Electronic Structure of Solids* (Eds.: P. Ziesche, H. Eischrig), Akademie Verlag, Berlin, **1991**. — [21c] J. Perdew, J. A. Chevary, S. H. Vosko, K. A. Jackson, M. R. Pederson, D. J. Singh, C. Fiolhais, *Phys. Rev. B* **1992**, *46*, 6671–6687.
- [22] deMon program: [22a] D. R. Salahub, R. Fournier, P. Mlynarski, I. Papai, A. St-Amant, J. Ushio, in *Density Functional Methods in Chemistry* (Eds.: J. Labanowski, J. Andzelm), Springer, New York, **1991**. — [22b] A. St-Amant, D. R. Salahub, *Chem. Phys. Lett.* **1990**, *169*, 387–392.
- [23] V. G. Malkin, O. L. Malkina, D. R. Salahub, *Chem. Phys. Lett.* **1996**, *261*, 335–345.
- [24] [24a] G. M. Sheldrick, *SHELXS-86, Program for Crystal Structure Solution*, University of Göttingen, Germany, **1986**. — [24b] G. M. Sheldrick, *SHELXL-93, Program for Crystal Structure Refinement*, University of Göttingen, Germany, **1993**.

Received April 5, 2000  
[100132]